THE ASTROPHYSICAL JOURNAL, 322:909–916, 1987 November 15

VLA AND LOW-FREQUENCY VLBI OBSERVATIONS OF THE RADIO SOURCE 0503 + 467: AUSTERE CONSTRAINTS ON INTERSTELLAR SCATTERING IN TWO MEDIA

STEVEN R. SPANGLER AND ALAN L. FEY
Department of Physics and Astronomy, University of Iowa

AND

JAMES M. CORDES
Astronomy Department, Cornell University
Received 1987 January 20; accepted 1987 May 4

ABSTRACT

The radio source 0503+467 lies near the Galactic plane ($l = 161°.0$, $b = 3°.7$) and at the edge of the supernova remnant (SNR) HB 9. Our VLA observations show that it has a spectrum typical of a compact extragalactic radio source. The resultant small angular size of the source makes it an excellent probe of turbulence in two media: the diffuse or "type A" component of interstellar turbulence and a hypothesized region of hydromagnetic turbulence upstream of the supernova remnant. An eight-station VLBI experiment at 326 MHz indicates that the source is less than about 20 milliarcseconds (mas) in angular diameter. A value of 16 mas is most appropriate as an upper limit to the interstellar scattering contribution to the measured angular size. The implications of this upper limit are twofold. First, the galactocentric radial scale to the type A turbulence is probably less than or equal to about 6 kpc. Second, no evidence is seen for shock-associated turbulence upstream of HB 9. Our measurements allow us to constrain a parameter which is a function of the rms density fluctuation in the upstream region, the outer scale to the density turbulence, and the thickness of the SNR foreshock region.

Subject headings: nebulae: supernova remnants — plasmas — turbulence

I. INTRODUCTION

In a previous paper, Spangler *et al.* (1986), hereafter Paper I, we reported multifrequency VLBI observations of five radio sources, apparently extragalactic, which lie near the Galactic plane. The purpose of those observations was to measure or constrain angular broadening of these sources due to the turbulent interstellar medium (ISM). The measurements could then be used to measure, or place limits on, the properties of electron density turbulence along the line of sight.

The five sources observed were chosen for their proximity to supernova remnants (SNRs). As discussed in Cordes, Weisberg, and Boriakoff (1985), interstellar turbulence appears to be of two types; the first consists of a ubiquitous, diffuse component and the second consists of regions of highly enhanced turbulence. Cordes, Weisberg, and Boriakoff refer to the first of these as the "type A" medium and the second as the "type B" medium. At present, we do not know the classes of astronomical objects with which the type B clumps are associated. In our study for Paper I, we were investigating the possibility that the vicinities of SNRs could be such regions of enhanced turbulence. The specific physical mechanism proposed for this association was the reflection of cosmic rays and other ions from the supernova shock. These reflected particles, streaming into the upstream ISM, would generate magnetohydrodynamic waves, which in turn would produce plasma density fluctuations.

The attractions of this suggestion are twofold. First, these phenomena have been extensively observed by spacecraft in the solar wind. At the Earth's bow shock we observe reflected ions, large-amplitude magnetohydrodynamic (MHD) waves, and plasma density fluctuations. Similar phenomena have been observed at other planetary shocks, traveling interplanetary shock waves, and the strong interaction regions of comets and the solar wind. It is obviously inviting to apply well-studied and reasonably understood physical processes to the ISM. Second, such a mechanism would produce, quite naturally, density fluctuations on the size scales required by interstellar scintillation observations. Furthermore, these interplanetary density fluctuations are of large amplitude. During two periods of observation in the Earth's foreshock, Spangler *et al.* (1987) found the rms density fluctuation to be of order 15% of the mean density. Further discussion of this mechanism is given in Paper I and in § III below. One must naturally be cautious in such a transportation of solar system microphysics to the ISM. Important parameters such as plasma β, ion-neutral collision frequencies, etc. can be quite different in the two plasmas. Nonetheless, the ubiquity of solar system foreshock phenomena encourages us to seek evidence of these processes in the ISM.

The results of Paper I were that two out of the five sources observed manifested the effects of interstellar scintillation. Indeed, one of these, 1849+005, appears to be so heavily scattered that it was totally resolved by our VLBI interferometers. Such a high degree of scattering is in excess of that observed for most lines of sight through the Galactic plane. An important role of the SNR G33.6+0.1 cannot, at present, be excluded, although the low Galactic longitude of this line of sight naturally allows many objects and media to furnish the enhanced scattering. It is of interest to note that a recently discovered pulsar (Clifton, Lyne, and Jones 1987), 10′ from 1849+005 and nearer the SNR, shows an extremely large amount of scattering that is consistent with the lower bound for 1849+005. The other source, 2013+370, is in a part of the sky characterized by heavy scattering, so it is difficult to assess the contribution from the SNR G74.9+1.2.

For the remaining three radio sources, interstellar scintillation was not definitely detected; only upper limits could be set to the amount of angular broadening attributable to the ISM. These upper limits placed interesting constraints on the properties of density turbulence upstream from the supernova shocks.

In this paper, we report new radio observations of one of the five sources, 0503+467. This source is of interest to both the study of density fluctuations upstream of supernova shocks and the study of general properties of interstellar turbulence. Of the five sources discussed in Paper I, 0503+467 is the closest to the adjacent SNR; the maps of Willis (1973, reproduced in Paper I) and Reich, Fürst, and Sieber (1983) show the source to be essentially blended with the limb of the remnant. To the authors' knowledge, this object represents the best case for the line of sight to a compact radio source passing through a supernova foreshock, without penetrating the interior of the remnant. It therefore may present our best opportunity to deduce characteristics of upstream waves and particles. Another desirable property of this source is that it was observed to be quite compact at 610 MHz, with an angular size of ~ 10 milliarcseconds (mas). The compact nature of this source makes observations sensitive to even small amounts of interstellar scattering.

Further observations of this object are of more general interest as well. With Galactic coordinates of $l = 161\overset{\circ}{.}0$, $b = 3\overset{\circ}{.}7$, the line of sight traverses a long path through the ISM. Cordes and Spangler (1987) have recently discussed the Galactic distribution of the "type A" turbulence component. As will be seen in § III, our observations provide an extremely important datum for this endeavor.

The new radio observations reported in this paper are of two types. The first consists of VLA observations. The purpose of the VLA observations was (*a*) to obtain a precise position for the source for use in subsequent VLBI observations, (*b*) to make flux density measurements at the four VLA frequencies so a radio spectrum could be assembled, and (*c*) to more precisely measure the angular separation of the radio source and limb of the SNR. The second type of radio observation undertaken consists of VLBI observations made at a low radio frequency of 326 MHz in order to take advantage of the λ^2 dependence of the "seeing disk" due to interstellar scattering.

II. ACQUISITION OF DATA AND OBSERVATIONAL RESULTS

a) VLA Observations

Observations with the Very Large Array[1] were made during an 8 hr period on 1985 July 23. The VLA at that time was in the "C" configuration. This configuration was chosen as a compromise between the needs of goals (*a*) and (*c*) listed in the previous section. Approximately 6 hr were spent in 20 cm observations to map the vicinity of 0503+467. The remaining time was spent in observing 0503+467 at the remaining three VLA bands and in measuring the position and flux density of 0455+458, a source viewed through the HB 9 SNR. The source DA 193 was monitored as a phase and secondary amplitude calibrator.

i) *Position of 0503+467*

The position of the source was taken as the mean of the 5 and 15 GHz positions. At 22 GHz, the angular resolution is higher, but phase stability is worse. At 1.4 GHz, phase stability is good, but the angular resolution is relatively poor. The positions were determined by a Gaussian fit to the cleaned maps. Our position for 0503+467 is

$$\alpha_{1950} = 5^{\mathrm{h}}03^{\mathrm{m}}40\overset{\mathrm{s}}{.}99 \pm 0.01 ,$$

$$\delta_{1950} = +46°41'46\overset{''}{.}35 \pm 0.10 .$$

The uncertainties quoted represent departures of the 5 and 15 GHz positions from the mean.

ii) *Spectrum of 0503+467*

At each VLA frequency of observation, the data were mapped and submitted to one iteration of *phase only* self-calibration. A Gaussian fit was made to the self-calibrated cleaned maps for the source flux. The source was unresolved to the VLA at all frequencies of observation.

We present our flux density measurements in Table 1. In addition to our present VLA measurements, we also list a 610 MHz VLBI measurement from Paper I, a 326 MHz VLBI measurement from this paper, and a 102 MHz interplanetary scintillation measurement from Pynzar and Udaltsov (1983). The data from Table 1 are plotted in Figure 1.

The results of Figure 1 show that 0503+467 has a spectrum characteristic of a compact extragalactic radio source. Above about 2 GHz the spectrum is describable by a spectral index of 0.15, while below this frequency it is approximately flat.

iii) *Map of the Vicinity of 0503+467*

As mentioned in the Introduction, the intention of this facet of the observing program was to detect compact features in the SNR shell which could be used to measure the angular separation of 0503+467 and the edge of the remnant. Considerable effort was expended to this end; data in two separate 50 MHz IF bandpasses were submitted to phase self-calibration, trial of various tapering functions in the (u, v)-plane, and finally registration and summing. These efforts were unsuccessful in obtaining compelling evidence for the edge of the SNR.

In Figure 2 we present our map of this region. The map was made with a $\lambda 5000$ taper in the (u, v)-plane and has a resolution of 25". We present the data for the benefit of those who might be interested in further investigations of these objects. Sources 1 and 2 may be identified on the single dish map of Reich, Fürst, and Sieber (1983). Although on the basis of the radio data we cannot identify any of these features as SNR emission, subsequent optical investigations might indicate whether these sources are Galactic or extragalactic. In Table 2, we therefore

TABLE 1

FLUX DENSITY DATA FOR 0503+467

Frequency (GHz)	Flux (Jy)	Source
22.3	0.500 ± 0.010	1
15.4	0.518 ± 0.010	1
4.9	0.617 ± 0.006	1
1.45	0.734 ± 0.007	1
0.610	0.9 ± 0.1	2
0.326	0.7 ± 0.1	3
0.102	0.8 ± 0.2	4

NOTE.—The numbers in the last column refer to the following sources: (1) VLA, This paper; (2) VLBI, Paper I; (3) VLBI, This paper; (4) IPS, Pynzar and Udaltsov 1983.

[1] The Very Large Array of the National Radio Astronomy Observatory is operated by Associated Universities, Inc., under contract from the National Science Foundation.

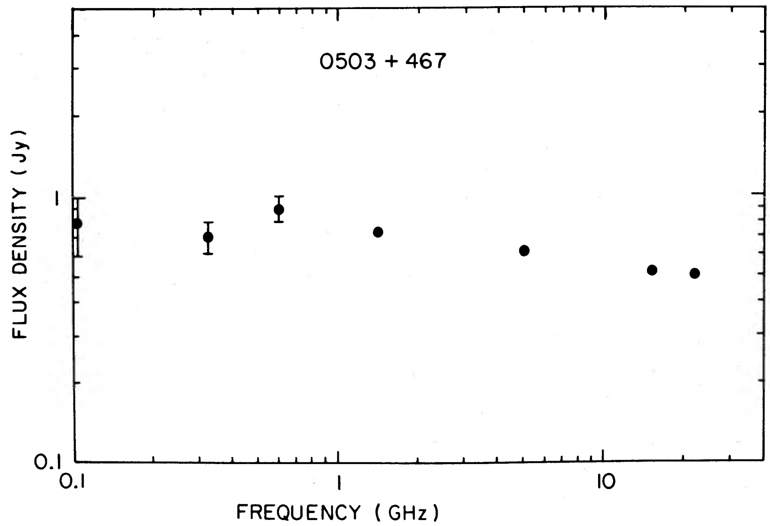

FIG. 1.—Radio spectrum of 0503+467. Measurements above 1 GHz are from VLA observations reported in this paper. VLBI observations provide flux densities at 326 and 610 MHz (see text). The 102 MHz observation is an IPS measurement by Pynzar and Udaltsov (1983).

list the positions and flux densities of the sources enumerated in Figure 2.

The positions in Table 2 were measured from untapered maps to obtain maximum resolution. Flux densities in the fourth column were obtained from heavily tapered maps, so these flux densities should represent total flux densities. For both types of measurements, Gaussian models were fitted in a least-squares sense to the features in the cleaned maps.

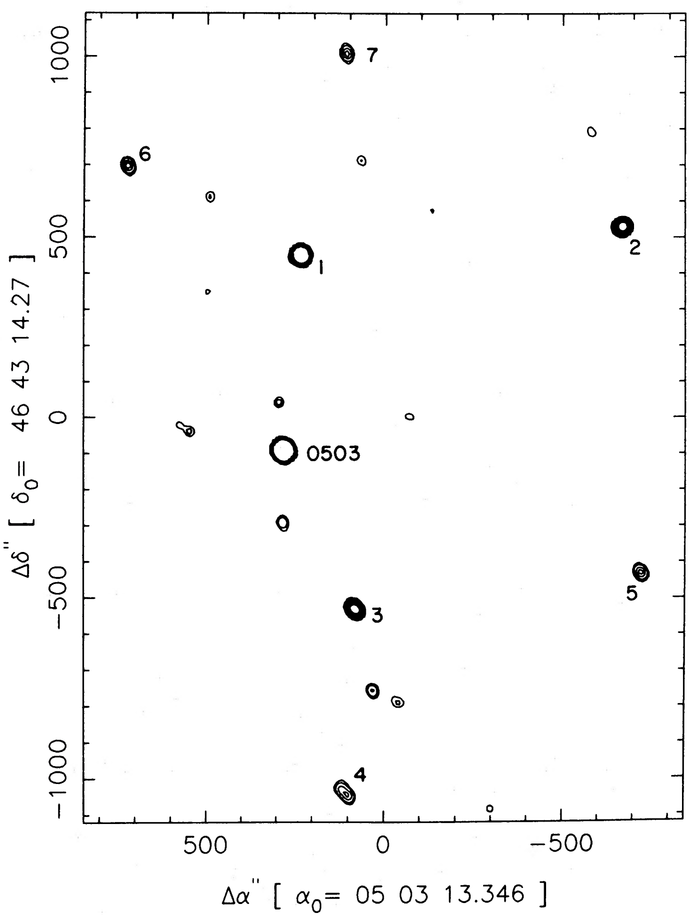

FIG. 2.—A 1.45 GHz map of the vicinity of 0503+467. Position and flux density data for numbered sources are given in Table 2. Angular resolution of the map (θ_{FWHM} of clean beam) is 25″. Contours are in units of 1.32, 2.20, 4.40, 6.60, 8.80, 10.99, 13.19, 15.39, 17.59, and 19.79 mJy per beam.

The final object listed in Table 2, 0455+458, lies outside the field of Figure 2. It may be seen clearly in the figure of Reich, Fürst, and Sieber (1983). This object was observed in short scans at 1.45 and 4.9 GHz, because it appears to be an extragalactic radio source viewed through an SNR. The object is unresolved at 6 cm and would appear to be suitable for radio observations intended to probe the interior of an SNR.

b) *326* MHz *VLBI Observations*

VLBI observations at a frequency of 326 MHz were made over a 14 hr period on 1986 March 23 and 24. The VLBI interferometer consisted of Jodrell Bank, Westerbork, Maryland Point, NRAO-Green Bank, Fort Davis, eight phased elements of the VLA, Owens Valley, and Hat Creek. Most of the time was spent observing 0503+467, but two brief periods were allocated to observing 0016+731, and one such period to

TABLE 2

POSITIONS AND FLUX DENSITIES OF SOURCES IN FIELD OF 0503+467

Source[a]	α_{1950}	δ_{1950}	$S_{1.4\ GHz}$ (Jy)
0503+467[b]	5ʰ03ᵐ40ˢ.99	46°41′46″.35	0.734
1	5 03 36.20	46 50 45.8	0.198
2	5 02 08.08	46 52 01.2	0.108
3[c]	5 03 22.01 5 03 21.06	47 34 31.4 46 34 22.9	0.041
4	5 03 23.79	46 25 56.3	0.016
5	5 02 03.43	46 36 00.8	0.020
6	5 04 23.73	46 54 49.7	0.016
7	5 03 23.84	47 00 02.3	0.023
0455+458[b,d]	4 55 50.79	45 48 18.56	0.421

[a] Sources are numbered as on Fig. 2.

[b] Position taken from higher resolution, 5 GHz maps.

[c] Source resolved as double.

[d] Source outside of field of Fig. 2, flux density at 5.0 GHz = 0.137 Jy.

observations of 0544+273. Brief descriptions of these latter observations will be given at the end of this section.

For calibration purposes, the pulsar 0329+54 was observed twice during this experiment. It is of low-dispersion measure and weakly scattered; it is therefore probably the most ideal point source to use for VLBI observations at this low frequency. Due to the brightness of this pulsar, it was not necessary to gate the recorders or correlator. The effective flux density of the pulsar was about 2.7 Jy. The flux of the pulsar was not independently measured during the observations, so we cannot determine the gains of the antennas in an absolute sense. However, by assuming the pulsar to be a point source, we can level the gains within the array. In any case, we believe the absolute calibration to be acceptable.

Fringe fitting was carried out by means of the global fringe-fitting technique (Schwab and Cotton 1983), as implemented in the NRAO AIPS software package. Experiments with the PSR 0329 data revealed a significant (30%) drop in the fringe amplitude on the longest baselines, apparently due to ionospheric effects, as the fringe-fitting time was increased from 30 s to 4 minutes. This finding necessitated the conservation of a short fringe-fitting time, highly undesirable in view of the weakness (0.8 Jy) of 0503+467.

Reduction and analysis of the data progressed by the following steps:

1. All available correlator data were used in the global fringe-fitting analysis. A solution interval of 4 minutes was chosen for determining the phase, fringe rate, and delay for each antenna. By the nature of the AIPS global fringe-fitting program, these delays and rates are applied to the original data set to "stop" the fringes, but the data are left in 2 s records.
2. The corrected 2 s records were averaged to intervals of 30 s to improve the signal-to-noise ratio for step 3 below.
3. The 30 s data were subject to a phase self-calibration procedure, with a point source as a model. The purpose of this step was to remove the fast ionospheric phase fluctuations responsible for the loss of coherence referred to above. Our hope was that at this point the fringes were stopped for long periods.
4. The 30 s data were averaged to 5 minute records to improve signal-to-noise ratio.
5. Data were edited and calibrated in the standard manner.
6. The visibility data were mapped and cleaned and Gaussian models were fit to the visibility data. The results of these analyses will be presented below.

i) *0503+467*

We now proceed to discuss our results on the 326 MHz structure of 0503+467. Our primary result is a map of this source, displayed in Figure 3. The resolution of the map, taken to be the dimension of the clean beam, is 21 mas FWHM. It is obvious from this map that the source is structurally simple and compact. This figure graphically presents the primary result of this paper; the source 0503+467 is quite compact at a low radio frequency, so there is relatively little scattering along the line of sight.

To obtain a quantitative measurement of the source angular size, a Gaussian model was fitted to the clean map, and the response of the clean beam deconvolved, leaving a Gaussian-equivalent angular size for the source. Two such calculations were carried out using different fitting windows. The results of the first fit for total source flux density, major axis and minor axis, and position angle of the two-dimensional Gaussian were

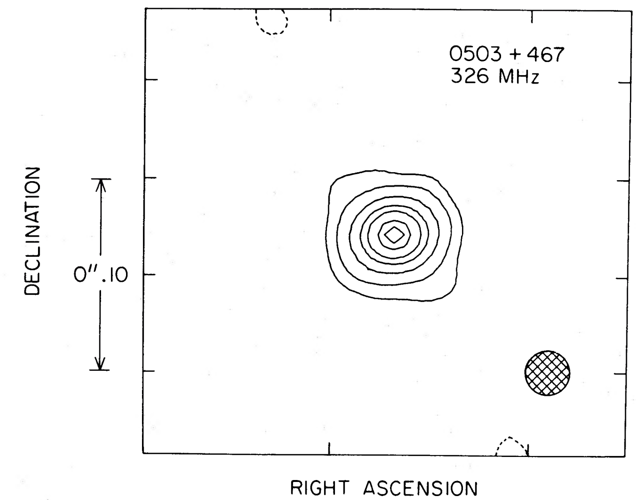

FIG. 3.—A 326 MHz VLBI map of radio source 0503+467. Clean beam is 21.5 mas, FWHM. Contours are at −5%, 5%, 10%, 20%, 35%, 50%, 75%, and 90% of peak brightness, which is 0.42 Jy per beam. Cross-hatched circle represents the diameter (FWHM) of the restoring beam.

0.64 Jy, 19 and 13 mas, and 92°, respectively. In the second calculation, using a larger fitting window, the fit parameters were 0.70 Jy, 23 and 17 mas, and 94°. The total cleaned flux for the map was 0.79 Jy. From the aforementioned measurements, we adopt a 326 MHz flux density of 0.70 ± 0.10 Jy, listed in Table 1 and plotted in Figure 1.

We also fitted Gaussian models to the visibility data and examined plots comparing these to the observed visibilities. The models so derived were in agreement with those described above. It is interesting to note that the correlated flux density on long baselines (e.g., Jodrell-OVRO) generally was in excess of that predicted by the best-fit Gaussian model.

The results of our observations may be summarized as follows. The angular diameter of the source, in the sense of a Gaussian FWHM, is 19–23 mas, with an axial ratio of about 0.7. Experiences from both fits to the source map and to the visibilities indicate that the structure departs from a Gaussian, in that the brightness is more centrally condensed. Said differently, the structure may be better described as a core-halo than as a single Gaussian. This point merits emphasis because in our analysis it is the angular size of the most compact source feature which yields information on interstellar scattering.

ii) *0544+273 and 0016+731*

To conclude this section, we briefly comment on our results for the radio sources 0544+273 and 0016+731. The first of these sources is of interest because the line of sight passes inside the outermost Hα filaments of the SNR S 147 and, therefore, samples the interior of an SNR. Prior VLBI observations, in 1985 February at a frequency of 4.99 GHz (US VLBI Network experiment S 45), detected the source. The structure at 5 GHz can be roughly described by a circular Gaussian of FWHM = 0.70 mas and 0.42 Jy total flux. The angular size is quite typical of compact extragalactic radio sources at these frequencies, and allows a limit, albeit not very restrictive, to be set on turbulence in the remnant interior. Our hope was to detect this source at 326 MHz, in which case scattering could be detected, or a restrictive upper limit produced. Unfortunately, no fringes were detected on any baselines, probably because of the weakness of the source.

Observations of the source 0016+731 at frequencies of 4.9, 1.7, and 0.61 GHz were reported in Paper I. This source is of interest by virtue of its proximity to the SNR CTA 1 and its location on the sky ($l = 120^\circ.6$, $b = 10^\circ.7$). The only baseline on which reliable fringes, capable of calibration, were obtained was NRAO-OVRO. The correlated flux was 0.3–0.4 Jy. This information is inadequate for analysis, but indicates that future low-frequency VLBI observations of this source, employing large antennas, might well be feasible.

III. INTERPRETATION AND DISCUSSION

a) *Adoption of the Scattering Angular Size for 0503+467*

In § II we presented our VLBI observations of 0503+467 and parameterized the structure of this source. We now wish to extract from these measurements an angular size which may be attributed to scattering in the ISM. It should be emphasized at the outset that we have an upper limit to the interstellar scattering of 0503+467. We cannot convincingly distinguish intrinsic from scattered structure for this object. Our analysis will therefore be primarily concerned with the consequences of the fact that the ISM did not broaden this source to a size greater than or equal to that measured.

Our analysis will deal with the Gaussian fits to the map shown in Figure 3. For reasons discussed in § II, we think it far more likely that the model with the smaller angular size is a better representation of the most compact portion of the source. Nonetheless, both estimates will be retained and will provide limits of different severity. Both fits yielded an asymmetric source structure with an axial ratio of about 0.7. Contrary to what might initially be thought, an asymmetric source image does not preclude the agency of interstellar scattering. Asymmetric scattering images can arise from refractive "squeezing" of the image (Cordes, Pidwerbetsky, and Lovelace 1986; Romani, Narayan, and Blandford 1986) or because the irregularities themselves are anisotropic (Higdon 1984). Since, as will be seen below, we believe that the observed structure is intrinsic and we desire a single number with which to describe the strength of scattering, we adopt angular sizes which are the harmonic mean of the major and minor axes of the corresponding Gaussian model. This convention is probably acceptable, even if the brightness distribution is mainly determined by scattering. For the two estimates of the source size we therefore have 19.8 and 15.7 mas.

Distinguishing intrinsic from scattered structure requires multifrequency observations and some knowledge about the intrinsic source structure. The results of Paper I provide limited structural information at another frequency (610 MHz), and the spectrum shown in Figure 1 allows some deductions to be made about the frequency dependence of the intrinsic source size.

We therefore undertook an analysis in which it was assumed that the source structure at any frequency is a convolution of an intrinsic image with an interstellar broadening function, with both assumed Gaussian. The measured size is then a quadratic sum of the intrinsic size and the scattering size. We know the scattering size is proportional to the square of the wavelength. Given the spectrum shown in Figure 1 and results from models of inhomogeneous synchrotron radiation sources (Marscher 1977), we would expect the intrinsic angular size of 503+467 to be proportional to wavelength at frequencies below about 2 GHz.

With such a model for the observed source angular size as a function of frequency, one can, in principle, distinguish intrinsic and scattering contributions to the source structure, given measurements at two frequencies. The results of such an exercise with our 326 and 610 MHz observations are as follows. If we use the larger of the two angular size estimates, $\theta_{326} = 19.8$ mas, we would deduce a scattering size of 7.6 mas at 326 MHz. There is no solution for the smaller of the 326 MHz angular size estimates, $\theta_{\rm obs} = 15.7$ mas. The significance of this is that the measured 610 MHz angular size, extrapolated to 326 MHz, exceeds the lower of the two values for the 326 MHz angular size. This exercise indicates that much, or all, of the measured 326 MHz size may well be intrinsic to this source, with a negligible contribution from scattering in the ISM.

To conclude this subsection, we shall choose three angular size values to use in the subsequent discussion. The first is the most generous upper limit to interstellar scattering that is compatible with the data. This limit, referred to as the *timens* limit, is intended to provide an indisputable bound on scattering in the ISM. We adopt the harmonic mean of the major and minor axes in the larger of the two model fits to the clean map, which gives us $\theta_{\rm TI} = 20$ mas. As discussed in § II, the *timens* angular size is almost certainly too large, as it does not account for the existence of a more compact component in the object. Our next estimate, referred to as the *aequus* angular size, is intended to be somewhat more restrictive, but nonetheless still a conservative estimate for the scattering size. We choose the harmonic mean of the major and minor axes in the smaller of the two Gaussian fits to yield $\theta_{\rm AE} = 16$ mas. Neither the *timens* or *aequus* estimates take into account the above discussion pointing out that the 610 MHz angular size is a substantial fraction of that at 326 MHz and that intrinsic, rather than scattering, effects probably dominate the measured size. Our final size estimate uses the immediately cited analysis to estimate the scattering contribution and represents the most restrictive result consistent with our data and common sense. In view of the uncertainties attendant on this estimate, we refer to it as the *audax* estimate and have $\theta_{\rm AU} = 8$ mas.

b) *Constraints on Turbulent Media*

In this section, we consider the implications of these three estimates for properties of plasma turbulence in two media: the foreshock of the SNR HB 9 and the "A Component," or diffuse phase of general interstellar turbulence. In making this comparison, we will make use of parameters introduced by Cordes and Spangler (1987).

We adopt customary convention and describe electron density turbulence by a spectrum of the form,

$$P_{\delta n}(q) = C_N^2 q^{-\alpha} , \quad q_0 \leq q \leq q_1 , \tag{1}$$

where q is the spatial wavenumber, q_0 and q_1 are the outer and inner scales of the turbulence, and C_N^2 is the normalization constant of the spectrum. We choose a value of $\alpha = 3.7$ as indicated by a number of studies of pulsar scintillations. The strength of scattering is determined by a parameter termed the *scattering measure*, SM, defined as

$$\mathrm{SM} = \int_0^L ds C_N^2(S) , \tag{2}$$

where L is in kpc and C_N^2 has units of $\mathrm{m}^{-20/3}$. Finally, the scattering measure is related to the angular size by (Cordes and Spangler 1987)

$$\mathrm{SM} = (\theta_{\rm FWHM}/\theta_0)^{5/3} \nu^{11/3} , \tag{3}$$

where $\theta_0 = 133$ mas and ν is in GHz.

Using equation (3), we find the following scattering measures corresponding to angular sizes for the *timens*, *aequus*, and *audax* limits: $SM_{TI} \leq 6.9 \times 10^{-4}$; $SM_{AE} \leq 4.8 \times 10^{-4}$; $SM_{AU} \leq 1.5 \times 10^{-4}$.

i) *Foreshock of HB 9*

We now wish to consider the consequences of the above limits for the characteristics of the HB 9 foreshock. The goal of these deliberations will be to comprehend the small amount of scattering of 0503+467. In qualitative terms, the weak broadening signifies one of three possibilities concerning the foreshock of HB 9: (1) it is possible that SNR foreshocks do not exist, in spite of the arguments for analogy to shocks in the interplanetary medium; (2) the turbulence in the foreshock may be sufficiently weak to preclude strong scattering; (3) the foreshock may be of such small extent that the line of sight passes well outside the region of significant density perturbation.

We now proceed to make quantitative constraints on the foreshock characteristics. It will be seen that possibilities (2) and (3) immediately above may be expressed in the same formula, equation (5) below.

The geometry of the situation is shown in Figure 4. Here we consider an SNR of radius R. The thickness of the foreshock is ΔR, and the impact parameter, or distance of closest approach of the line of sight to the SNR shell, is y. The path length within the foreshock, S, is then given by:

$$S = 2^{3/2} R \sqrt{\left(\frac{\Delta R}{R}\right) - \left(\frac{y}{R}\right)}, \quad (4)$$

valid if $\Delta R/R$ and $y/R \ll 1$.

The parameter y/R may be directly measured from radio maps. From the map of Reich, Fürst, and Sieber (1983), we estimate $y/R \leq 0.035$. The remnant radius, R, can similarly be measured from maps. For an assumed distance of 1.1 kpc (Willis 1973) to this remnant, we measure its radius to be 22 pc. The fractional thickness of the foreshock, $\Delta R/R$, is unknown, and indeed observations of the type presented in Paper I and this paper constitute perhaps the only information obtainable on this parameter. If $\Delta R/R \leq 3.5\%$, the line of sight passes outside the foreshock and our observations tell us nothing about this region. However, if $\Delta R/R$ is even marginally in excess of y/R, the path length S is several parsecs. For example, if $\Delta R/R = 0.05$, $S = 7.7$ pc, and if $\Delta R/R = 0.10$, $S = 15.8$ pc.

A formula relating scattering size to turbulence properties, appropriate for a Kolmogorov density irregularity spectrum, was presented in equation (5) of Paper I. Adapting this formula to our present application, and using equation (4), we have the following relationship between the angular size measurement, θ_{326} (in mas), and σ_n (the rms density fluctuation in cm^{-3}), $\Delta R/R$, and L_0, (the outer scale of the turbulence in cm):

$$\frac{\sigma_n^{1.2}[(\Delta R/R) - 0.035]^{0.3}}{L_0^{0.4}} = 1.1 \times 10^{-10} \theta_{326} . \quad (5)$$

In obtaining equation (5), we have assumed a remnant radius of 22 pc and a fractional impact parameter, $y/R = 0.035$.

Equation (5) allows quantitative constraints to be placed on two of the three possibilities for weak scattering which were listed at the beginning of this subsection. With respect to the third of these possibilities, that the foreshock is of limited spatial extent, equation (5) immediately tells us that if the foreshock thickness is less than about 3.5% of the remnant radius, our line of sight would miss the foreshock region. We next wish to quantitatively enunciate the second of the possibilities, that the foreshock turbulence is weak.

We will assume that the foreshock thickness is 5% of the remnant radius. The weak dependence of the remaining quantities on the difference $[(\Delta R/R) - y/R]$ means that our analysis will be valid for a wide range of values of $\Delta R/R$, provided this ratio is in excess of y/R.

We also have some constraints on σ_n for the SNR HB 9. From an analysis of the X-ray emission of this object, Tuohy, Clark, and Garmire (1979) deduce that the expansion speed of the HB 9 remnant is 550 km s^{-1} and that it is expanding into a medium with density = 0.03 cm^{-3}.

Figure 5 reveals the way in which our observations and the immediately aforementioned properties of the HB 9 SNR constrain properties of turbulence in the remnant foreshock. The ordinate is the 326 MHz angular size predicted by equation (5). The abscissa is the outer scale of the turbulence in the foreshock. Dashed horizontal lines represent the *timens*, *aequus*, and *audax* estimates of the scattering size. The curves represent the scattering size predicted by equation (5) for three values of the rms density fluctuation. The rightmost curve, for $\sigma_n = 0.01$, corresponds to a highly turbulent foreshock in which the rms density fluctuation is equal to 33% of the mean. The middle curve represents the scattering diameter relationship if the rms density fluctuation is equal to 15% of the mean density, as is

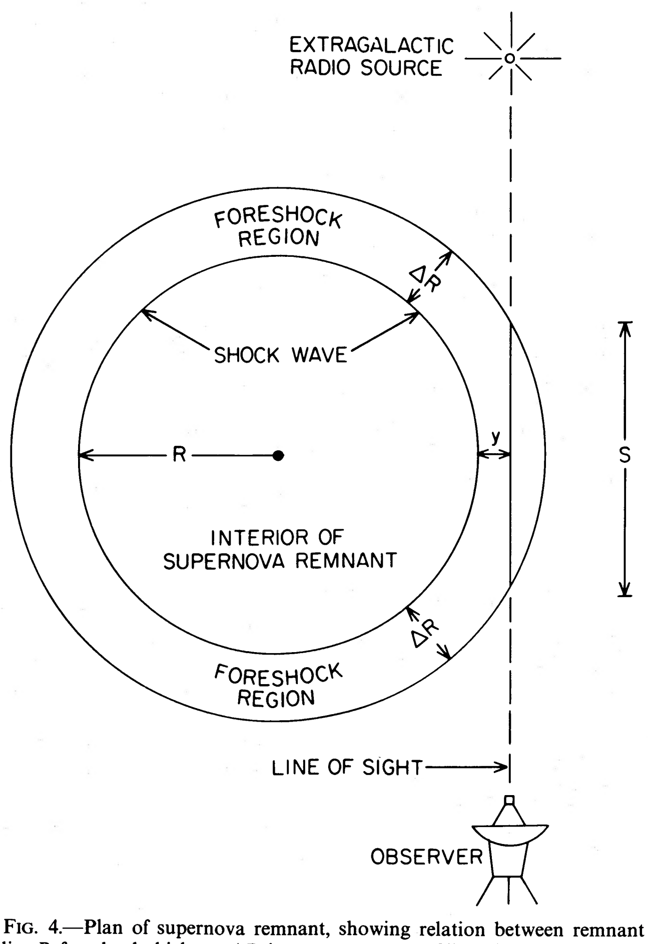

FIG. 4.—Plan of supernova remnant, showing relation between remnant radius R, foreshock thickness ΔR, impact parameter of line of sight y, and path length through the foreshock region S.

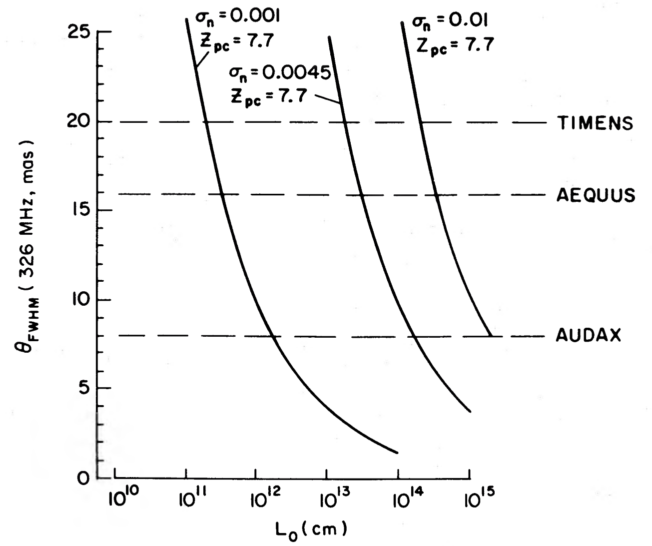

FIG. 5.—Plot of 326 MHz interstellar scattering size as a function of turbulence outer scale. Three solid curves correspond to three values of rms density fluctuation. Horizontal dashed lines represent three observational estimates of scattering size.

typical for the region upstream of the Earth's foreshock. The final curve corresponds to $\sigma_n = 0.001$, 3.3% of the mean density, and would indicate very weak small-scale turbulence.

These curves provide interesting constraints on the outer scale of SNR foreshock turbulence. Choosing the *aequus* limit for purposes of illustration, we see that if the rms density fluctuation is of order 15% of the mean, the outer scale must be $\gtrsim 3 \times 10^{13}$ cm. If the weak turbulence model, with $\sigma_n = 0.001$ cm^{-3} is appropriate, the outer scale is $\gtrsim 3 \times 10^{11}$ cm.

In discussing the significance of these limits, we again emphasize that we are primarily interested in searching for density fluctuations associated with MHD waves. Such fluctuations exist on scales comparable to the wavelength of MHD waves, which are vastly smaller than the "global" scales of an astrophysical plasma.

The wavelengths of the MHD waves we are considering are determined by a cyclotron resonance of streaming ions and the waves themselves, which is given by

$$\lambda \approx \frac{2\pi v_b}{\Omega_i}\,, \tag{6}$$

where v_b is the speed of the reflected ion beam and Ω_i is the ion-cyclotron frequency. Applying this formula to the ISM in the vicinity of HB 9, and assuming, as is the case for the Earth's bow shock, that the reflected ions travel back upstream at 2–3 times the shock speed, equation (6) predicts that MHD waves in the HB 9 foreshock should have wavelengths of about 10^{10} cm.

An empirical study by Spangler *et al.* (1987) of density fluctuations in the Earth's foreshock showed that fluctuations on scales from the MHD wavelength to 10–15 times the wavelength produced aggregate fluctuations with a modulation index of about 15%.

Employing this information from solar wind studies, we therefore expect SNR foreshock density fluctuations to be on scales of roughly 10^{10}–5×10^{11} cm. Consultation of Figure 5 shows that such outer scales are barely compatible with the *aequus* size for a miniscule modulation index of 3% ($\sigma_n =$ 0.001). For a solar wind analog model in which $\sigma_n/\bar{n} = 0.15$, our lower limits to the outer scale are at least 2 orders of magnitude greater than the scale on which MHD wave–generated density fluctuations should be occurring.

The results of Figure 5 and the preceding discussion may be summarized as follows: the source is far more compact (unblurred) than it should be, given that its radiation has probably traversed the foreshock of an SNR.

Of the possible explanations for the weak scattering given at the beginning of this section, we feel the most likely is that the line of sight to 0503+467 has passed outside the foreshock of HB 9, their celestial proximity notwithstanding. For this to be the case, it is necessary that the foreshock thickness be less than about 3.5% of the remnant radius or < 0.8 pc. This suggestion emphasizes the desirability for renewed VLBI observations of the source 0544+273; the line of sight to this source must perforate the foreshock of the remnant S147.

ii) *The Type A Component of Interstellar Turbulence*

It is arguable whether the line of sight to 0503+467 passes through the foreshock of the SNR HB 9. There is no question that it traverses the general ISM and is affected by turbulence therein.

As noted in § I, Cordes, Weisberg, and Boriakoff (1985) demonstrated that interstellar turbulence is constituted of intense clumps embedded in a diffuse medium. Our observations of 0503+467 are relevant to this diffuse or type A medium. Scattering data for nearby or high-latitude pulsars point to a consistent value of $C_N^2 \approx 10^{-3.5}$. Additional studies by Cordes and Spangler (1987), utilizing pulsar and extragalactic source data, indicate that the z (distance above the Galactic plane) scale height of this turbulence is ~ 500 pc.

To compete a "first-order" model of the A turbulence, we need some information concerning its dependence on galactocentric distance. As discussed in Cordes and Spangler (1987), angular broadening measurements of low-latitude extragalactic sources furnish the best constraints on the radial distribution of turbulence.

Cordes and Spangler (1987) consider the following model for the Galactic distribution of type A turbulence:

$$C_N^2(r, z) = C_{N0}^2 e^{-r^2/A^2} e^{-|z|/H}\,, \tag{7}$$

where r is the radial distance from the Galactic center and z is the height above the Galactic plane. The quantities A and H are, respectively, the scales in galactocentric distance and height above the Galactic plane. Cordes and Spangler (1987) give an expression (eq. [7] of their paper) for the scattering measure to an extragalactic source, given a turbulence distribution of the form of equation (7).

For extragalactic sources at low latitudes, the scattering measure is only weakly sensitive to the scale height H, which in any case is well specified by the pulsar observations. Pulsar observations also provide us with an accurate measurement of C_{N0}^2 (actually $C_{N0}^2 e^{-(R_0/a)^2}$, where R_0 is the galactocentric distance of the Sun) and thus the local value of the type A C_N^2. As a consequence, low-latitude extragalactic source observations provide unambiguous information on the radial scale, A.

Equation (7) of Cordes and Spangler (1987) was used to calculate the scattering measure as a function of A for the Galactic coordinates of 0503+467. We adopted a local $C_N^2 = 10^{-3.5}$ and a scale height $H = 0.5$ kpc. Equation (3) was then used to convert these scattering measures to 326 MHz angular sizes.

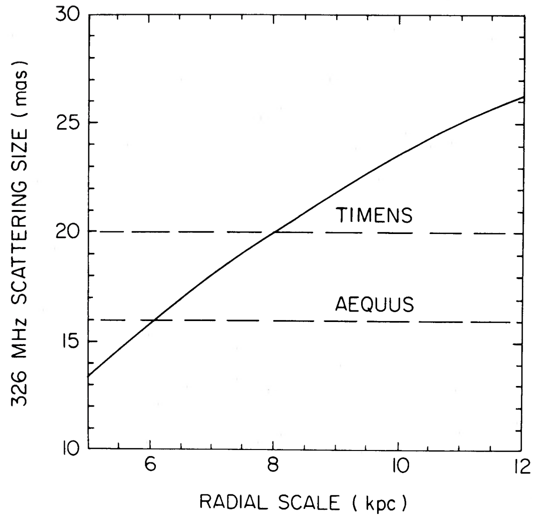

FIG. 6.—Solid curves show the 326 MHz scattering size, due to type A turbulence, as a function of radial scale of this turbulence. Horizontal dashed lines represent three observational estimates of scattering size.

The results are shown in Figure 6. The abscissa is the radial scale A in kpc. The ordinate is the scattering angular diameter (FWHM) at 326 MHz; precisely the quantity emergent from our observational studies. Horizontal lines delineate the *timens* and *aequus* observed scattering size estimates. Figure 6 demonstrates that our observations furnish quite stringent limits on the radial distribution of type A turbulence. If we choose the *timens* estimate, we conclude that the radial scale is about 8 kpc. The more likely *aequus* limit indicates that this scale is about 6 kpc. Again, recognition of the fact that the *timens* and *aequus* estimates are probably upper limits leads us to a rather small value for the radial scale. Furthermore, as is obvious from Figure 6, adoption of the *audax* estimate would lead to a radial scale so small as to invalidate the model, equation (7). We conclude that whatever the nature of the type A turbulence, it is extinguished not far beyond the orbit of the Sun.

IV. CONCLUSIONS

Our conclusions are as follows:

1. VLA and 326 MHz VLBI observations have been made of the extragalactic radio source 0503+467. Its spectrum is typical for a compact extragalactic source, flattening due to synchrotron self-absorption at a frequency of about 1 and 2 GHz. The flux density in the low-frequency regime is ≈ 0.8 Jy. Above 2 GHz, the flux density decreases with a spectral index of ~ 0.15.

The source is quite compact at 326 MHz. The structure may be parameterized as a Gaussian of major axis 19–23 mas, axial ratio of about 70%, and position angle near 90°.

2. The small angular size of this source severely constrains interstellar scattering along the line of sight to this object. Since 0503+467 is at Galactic coordinates $l = 161°.0$, $b = 3°.7$ and adjacent to the SNR HB 9, our observations provide constraints on the properties of turbulence in the foreshock of HB 9, as well as in the general ISM. The line of sight does not seem to have encountered an extensive region of turbulence similar to that observed near solar system shocks; such might well have been expected for the ISM adjacent to an SNR. The observations constrain the product $\sigma_n^{1.2}[(\Delta R/R) - 0.035]^{0.3}/L_0^{0.4}$ to be less than about 1.8×10^{-9} (employing the *aequus* limit), where σ_n is the rms electron density fluctuation (cm^{-3}), L_0 is the outer scale to the turbulence (cm), and $\Delta R/R$ is the thickness of the foreshock normalized by the remnant radius. In our opinion, the most likely explanation is that the thickness of the foreshock is less than about 3.5% of the remnant radius. Alternatively, the density turbulence may be considerably weaker than that observed near solar system foreshocks. This represents one of the first solid observational results relating to SNR foreshocks.

The same observational limit also constrains the (galactocentric) radial extent of the general, or type A, interstellar turbulence. Our best estimate is that the galactocentric radial scale is less than, or of order, 6 kpc. This implies that the type A turbulence does not extend far beyond the orbit of the Sun.

A portion of this work was accomplished while S.R.S. was a visitor at the Istituto di Radioastronomia in Bologna. He wishes to thank his Bolognesi colleagues and the Italian Consiglio Nazionale Delle Richerche for an exceedingly pleasant and productive period. This research was supported at the University of Iowa by grants NAGW-806 and NAGW-831 from the National Aeronautics and Space Administration. At Cornell University, the work was supported by the Alfred P. Sloan Foundation, NSF grant AST-8520530, and by the National Astronomy and Ionosphere Center, which is funded by a contract between Cornell University and the National Science Foundation.

REFERENCES

Clifton, T. R., Lyne, A., and Jones, B. 1987, in preparation.
Cordes, J. M., Pidwerbetsky, A., and Lovelace, R. V. E. 1986, *Ap. J.*, **310**, 737.
Cordes, J. M., and Spangler, S. R. 1987, submitted to *Ap. J.*
Cordes, J. M., Weisberg, J. W., and Boriakoff, V. 1985, *Ap. J.*, **288**, 221.
Higdon, J. C. 1984, *Ap. J.*, **285**, 109.
Marscher, A. P. 1977, *Ap. J.*, **216**, 244.
Pynzar, A. V., and Udaltsov, V. A. 1983, *Soviet Astr.*, **27**, 286.
Reich, W., Fürst, E., and Sieber, W. 1983, in *IAU Symposium 101, Supernova Remnants and Their X-Ray Emission*, ed. J. Danziger and P. Gorenstein (Dordrecht: Reidel), p. 377
Romani, R. W., Narayan, R., and Blandford, R. 1986, *M.N.R.A.S.*, **220**, 19.
Schwab, F. R., and Cotton, W. D. 1983, *A.J.*, **88**, 688.
Spangler, S. R., Fuselier, S., Fey, A. L., and Anderson, G. 1987, submitted to *J. Geophys. Res.*
Spangler, S. R., Mutel, R. L., Benson, J. M., and Cordes, J. M. 1986, *Ap. J.*, **301**, 312 (Paper I).
Tuohy, I. R., Clark, D. H., and Garmire, G. P. 1979, *M.N.R.A.S.*, **189**, 59P.
Willis, A. G. 1973, *Astr. Ap.*, **26**, 237.

JAMES M. CORDES: Astronomy Department, Cornell University, Space Sciences Building, Ithaca, NY 14850

STEVEN R. SPANGLER and ALAN L. FEY: Department of Physics and Astronomy, The University of Iowa, Iowa City, IA 52242